Multidimensional quasiballistic thermal transport in transient grating spectroscopy

A. J. Minnich

Multidimensional quasiballistic thermal transport in transient grating spectroscopy

A. J. Minnich[1, *]

[1]*Division of Engineering and Applied Science*
California Institute of Technology
Pasadena, CA 91125

Abstract

Transient grating spectroscopy has emerged as a useful technique to study thermal phonon transport because of its ability to perform thermal measurements over length scales comparable to phonon mean free paths (MFPs). While several prior works have performed theoretical studies of quasiballistic heat conduction in transient grating, the analysis methods are either restricted to one spatial dimension or require phenomenological fitting parameters. Here, we analyze quasiballistic transport in a two-dimensional transient grating experiment, in which heat conduction can occur both in- and cross-plane, using an analytic Green's function of the Boltzmann equation we recently reported that is free of fitting parameters. We demonstrate a method by which phonon MFPs can be extracted from these measurements, thereby extending the MFP spectroscopy technique using transient grating to opaque bulk materials.

I. INTRODUCTION

Transient grating spectroscopy (TG) is a noncontact, optical pump-probe experiment that is capable of measuring the in-plane thermal conductivity of thin films and bulk materials.[1,2] In this experiment, the sample is impulsively heated with a spatially sinusoidal temperature profile created by splitting a pump laser pulse using diffractive optics and recombining the beams on the sample. A probe laser subsequently observes the in-plane transient thermal decay by measuring the intensity of light diffracted from the sample surface. In the heat diffusion regime, the shape of the transient decay curve is controlled by the in-plane thermal diffusivity,[2] and thus the thermal diffusivity can be measured from the exponential time constant of the thermal decay.

Recently, considerable interest has focused on quasiballistic heat conduction in TG, in which phonon mean free paths (MFPs) are comparable to the grating period.[3–8] Prior works have demonstrated that observations of thermal transport in this regime yield information about the MFP spectrum of thermal phonons in a technique known as MFP spectroscopy.[5,7] A number of models have been proposed to explain these results, including a two-fluid model,[5] a two-parameter nondiffusive model,[3] and related models for time-domain thermoreflectance experiments.[9–12] Recently, we reported an exact analytic solution of the Boltzmann transport equation (BTE) for 1D transport in TG.[8]

However, often the thermal transport induced by the pump pulse is not purely 1D due to the finite optical penetration length of light in the sample.[2] For example, applying TG to a GaAs wafer generates the externally defined in-plane grating but also an exponential decay in the cross-plane direction, resulting in both cross-plane and in-plane heat conduction and a thermal decay that is no longer a pure exponential.[13,14] While in the diffusive case these measurements can be readily interpreted with Fourier's law,[13] in the quasiballistic regime interpreting the thermal decays is difficult because a unique thermal time constant can no longer be clearly identified.

In this work, we provide a theoretical framework for treating multidimensional heat conduction in TG based on an analytic Green's function for the BTE we recently reported.[15] We find that the transport in 2D TG is considerably more complicated than that in 1D because the heating profile contains a spectrum of spatial frequencies rather than a single spatial frequency as in the 1D case. Nevertheless, we demonstrate a method to recover the

MFP spectrum from these measurements without any fitting parameters or knowledge of the MFPs. This work extends the capability of MFP spectroscopy using TG from thin films to bulk opaque solids.

II. THEORY

A. Boltzmann Equation

We begin by briefly reviewing the derivation of the multidimensional Green's fuction to the BTE as reported by Hua and Minnich.[15] The BTE under the relaxation time approximation is given by:

$$\frac{\partial g_\mathbf{k}}{\partial t} + \mathbf{v} \cdot \nabla_\mathbf{r} g_\mathbf{k} = -\frac{g_\mathbf{k} - g_0(T(\mathbf{r}, t))}{\tau_\mathbf{k}} + Q_\mathbf{k}, \tag{1}$$

where $g_\mathbf{k} = \hbar\omega(f_\mathbf{k}(\mathbf{r}, t, \mathbf{k}) - f_0(T_0))$ is the desired deviational distribution function, $Q_\mathbf{k}(\mathbf{r}, t)$ is the spectral volumetric heat generation, $\mathbf{v}$ is the phonon group velocity, $\tau_\mathbf{k}$ is the phonon relaxation time, and $\mathbf{k}$ is the phonon wavevector in phase space. $g_0(T(\mathbf{r}, t))$ is the local equilibrium deviational distribution function and is given by:

$$g_0(T(\mathbf{r}, t)) = \hbar\omega(f_{BE}(T(\mathbf{r}, t)) - f_0(T_0)) \approx C_\mathbf{k}\Delta T(\mathbf{r}, t). \tag{2}$$

assuming a small temperature rise $\Delta T(\mathbf{r}, t) = T(\mathbf{r}, t) - T_0$ relative to a reference temperature T_0. Here, $\hbar$ is the reduced Planck constant, $\omega(\mathbf{k})$ is the phonon frequency given by the dispersion relation, $f_{BE}(T(\mathbf{r}, t))$ is the local Bose-Einstein distribution, $f_0(T_0)$ is the Bose-Einstein distribution at T_0, and $C_\mathbf{k} = k_B(\chi/\sinh(\chi))^2$ is the mode specific heat, where $\chi = \hbar\omega(\mathbf{k})/2k_B T_0$. To close the problem, energy conservation is used to relate $g_\mathbf{k}$ to $\Delta T(\mathbf{r}, t)$ as

$$\sum_\mathbf{k} \left[\frac{g_\mathbf{k}}{\tau_\mathbf{k}} - \frac{C_\mathbf{k}}{\tau_\mathbf{k}}\Delta T(\mathbf{r}, t) \right] = 0, \tag{3}$$

where the sum is performed over all phonon modes in the Brillouin zone.

An analytic solution to the above equations is obtained by performing a Fourier transform over space and time in Eq. 1, substituting the result into Eq. 3, and solving for the temperature response $\Delta\widetilde{T}(\eta, \xi_x, \xi_y, \xi_z)$, where η and ξ_x, ξ_y, ξ_z are the Fourier variables in the time and spatial domains, respectively. This procedure assumes that the thermal transport occurs in an infinite domain so that a Fourier transform can be performed. The result for an isotropic crystal is:

$$\Delta\widetilde{T}(\eta, \xi_x, \xi_y, \xi_z) = \frac{\int_0^{\omega_m} \frac{\widetilde{Q}_{\mathbf{k}}(\eta, \xi_x, \xi_x, \xi_z)}{\Lambda_\omega \xi} \tan^{-1}\left(\frac{\Lambda_\omega \xi}{1+i\eta\tau_\omega}\right) d\omega}{\int_0^{\omega_m} \frac{C_\omega}{\tau_\omega}\left[1 - \frac{1}{\Lambda_\omega \xi}\tan^{-1}\left(\frac{\Lambda_\omega \xi}{1+i\eta\tau_\omega}\right)\right] d\omega}, \tag{4}$$

where the magnitude of spatial frequency $\xi = \sqrt{\xi_x^2 + \xi_y^2 + \xi_z^2}$. In the weakly quasiballistic regime where $\eta\tau_{\mathbf{k}} \ll 1$, the result can be simplified by expanding all terms in powers of $\eta\tau_{\mathbf{k}}$ and keeping only linear terms. The result is:

$$\Delta\widetilde{T}(\eta, \xi_x, \xi_y, \xi_z) = \frac{\widetilde{Q}(\eta, \xi_x, \xi_x, \xi_z)}{i\eta C + \kappa(\xi)\xi^2} \tag{5}$$

where $\widetilde{Q}(\eta, \xi_x, \xi_x, \xi_z)$ is the heating profile summed over all phonon wavevectors and $\kappa(\xi)$ is the apparent thermal conductivity that depends only on ξ, reflecting the isotropy of the crystal. The apparent thermal conductivity is given by:

$$\kappa(\xi) = \int_0^\infty f(\Lambda)S(Kn)d\Lambda \tag{6}$$

$$S(Kn) = \frac{3}{Kn^2}\left(1 - \frac{\tan^{-1}Kn}{Kn}\right) \tag{7}$$

where $f(\Lambda)$ is the MFP distribution, Λ is the MFP, $S(Kn)$ is the suppression function, and the Knudsen number $Kn = \xi\Lambda$. These results follow directly from the solution of the BTE and are valid for isotropic crystals and assuming that $\eta\tau_{\mathbf{k}} \ll 1$.

We now specialize this result for the 2D TG experiment. Along the in-plane, or x direction, the heating profile is a sinusoid with spatial frequency ξ_x. Along the cross-plane, or y direction, the heating profile is a decaying exponential with decay length β_1 corresponding to the optical depth for the pump beam in the solid. The probe beam samples this temperature profile with an optical depth β_2 corresponding to the probe wavelength. The heating along the z direction is uniform and hence $\xi_z = 0$. Recalling the expression for the Fourier transform of a decaying exponential, the temperature profile in 2D TG can thus be written as:

$$\Delta\widetilde{T}(\eta, \xi_x) = A\int_0^\infty \frac{(\beta_1^2 + \xi_y^2)^{-1}(\beta_2^2 + \xi_y^2)^{-1}}{i\eta C + \kappa(\xi)\xi^2}d\xi_y \tag{8}$$

where A is an arbitrary constant. This equation can be easily converted to the time domain as:

$$\Delta T(t, \xi_x) = A' \int_0^\infty \frac{\exp(-\alpha(\xi)\xi^2 t)}{(\beta_1^2 + \xi_y^2)(\beta_2^2 + \xi_y^2)} d\xi_y \tag{9}$$

where $\alpha(\xi) = \kappa(\xi)/C$ is the apparent thermal diffusivity and $A' = A/C$.

Equation 9 shows that the transient temperature profile for a 2D grating is a multiexponential decay with a spectrum of time constants determined by the apparent thermal conductivities. The relative contribution of each exponential decay to the total signal is weighted by the Fourier transform of the cross-plane heating profile. This situation is considerably more complicated than in the 1D case, for which the sole spatial frequency in the problem is externally defined by the grating period. In the 1D case, a single apparent thermal conductivity can be identified from the exponential time constant of the observed thermal decay for a specific grating period, and a set of thermal conductivities versus grating period can then be used to directly recover the MFP spectrum.[7] The transport can be considered 1D if the total spatial frequency $\xi = \sqrt{\xi_x^2 + \xi_y^2}$ is dominated by the in-plane spatial frequency ξ_x. More precisely, if $\xi_y^2/\xi_x^2 \lesssim 0.1$, tranport in the cross-plane direction can be neglected, indicating that the optical penetration depth should be at least three times greater than the grating period to neglect cross-plane transport.

If this requirement is not satisfied and the transport is 2D, the thermal decay is no longer a single exponential but a multiexponential. Such multiexponential decays occur often in science, for example in time-resolved measurements of fluorescent decays,[16] and are challenging to interpret because recovering all the exponential time constants from a multiexponential decay is an ill-posed problem for which a unique solution does not exist. Thus in the 2D case, an inverse problem must be solved to recover the apparent thermal conductivities from the measured temperature decays before any further information about the thermal phonons can be extracted. Further, the inverse problem is nonlinear because the function to be recovered is inside an exponential.

B. Optimization Problem

This inverse problem can be solved using constrained nonlinear optimization methods, thereby yielding the apparent thermal conductivities as a function of spatial frequency ξ. These values can then be directly used as input to the original inverse problem of recovering the MFP spectrum described in Ref.[7] that is readily solved using convex optimization.

The present inverse problem is to recover the function $\alpha(\xi)$ from a set of transient thermal decays, $\Delta T(t, \xi_x)$, where the spatial frequency along the in-plane direction ξ_x can be externally controlled by varying the grating period. The optical decay lengths β_1 and β_2 are assumed to be fixed by the material and optical wavelengths used in the experiment, thereby specifying the spatial frequencies along the cross-plane direction, ξ_y. This prototypical problem has been addressed using a number of methods in the past, including Prony's method,[17] Fourier methods,[18] and linearization to enable linear optimization algorithms.[16,19,20] In this work, we use nonlinear optimization methods to solve the problem because these algorithms are implemented in standard software packages such as MATLAB. Other approaches such as Bayesian methods may also be effective in solving this type of inverse problem.[21]

Let us discretize this problem by assuming with have N transient data sets $\Delta T_i(t, \xi_{x,i})$ corresponding to different grating periods used in the experiment. Our goal is to adjust M apparent thermal diffusivities α_j that depend on spatial frequency to match Eq. 9 to the experimental data set. This problem can be classified as a nonlinear constrained optimization by defining a cost function that measures the difference between the simulated and actual thermal decays and attempting to minimize this cost function by varying α_j. As with many inverse problems, attempts to solve this problem without any constraints will likely not succeed because a unique solution does not exist. The desired solution can only be recovered from the measurements if known physical facts about the solution are incorporated into the optimization.

Fortunately, a number of facts are known about the solution. Since the first derivative of the suppression function is always negative, $d\alpha/d\xi < 0$ for all spatial frequencies. The second and third derivatives of the suppression function contain regions of positive and negative values, and hence higher-order derivatives of $\alpha(\xi)$ are not necessarily always negative or positive. However, by plotting the second derivative of the suppression function, we observe that the only region where the second derivative of the suppression function is negative is for sufficiently small spatial frequencies such that traditional Fourier theory is an accurate model for the heat conduction. Hence, for spatial frequencies corresponding to the quasiballistic regime, $d^2\alpha/d\xi^2 > 0$. By similar reasoning, $d^3\alpha/d\xi^3 < 0$. These constraints can be implemented by approximating the derivative with finite differences and incorporating the resulting equations into the optimization as linear inequality constraints.

Second, the solution cannot have jumps between adjacent α_j that are too large. Consid-

ering that the spatial frequencies ξ_j are uniformly spaced, the maximum difference between α_{j+1} and α_j is:

$$\alpha_j - \alpha_{j+1} = \int_0^\infty \alpha(\Lambda)\left(-\frac{dS}{dKn}\right)\Lambda d\Lambda \Delta\xi \lesssim \alpha_{bulk}\Lambda_{med}\Delta\xi \tag{10}$$

where $\alpha(\Lambda) = \kappa(\Lambda)/C$ is the differential thermal diffusivity distribution versus MFP and Λ_{med} is an estimate of the median MFP of the material. This constraint can also be incorporated into the optimization as a linear inequality constraint.

Third, the apparent thermal diffusivities for many materials are contained within a known range and do not vary substantially over the range of experimentally attainable grating periods. Thus, upper and lower bounds on the allowed values of α_j can be imposed. For instance, for the analysis performed for Si in the next section, the apparent thermal diffusivities must be between 1 and 100 mm^2/s. Similar bounds can be imposed for other solids for which basic knowledge of bulk thermal properties is known.

With these constraints, the optimization problem can be solved with standard optimization routines in MATLAB. We use the *fmincon* function in MATLAB for this work. The cost function to be minimized is defined as the magnitude of the difference between the calculated and measured temperature decays for N different grating periods ξ_x. The constraints described above are put into matrix form and included in the optimization as linear inequality constraints. The outputs of the optimization are M discrete values of the function $\alpha(\xi_i)$ that minimize the cost function while satisfying the constraints.

III. RESULTS

To demonstrate the reconstruction, we first synthesize temperature decay curves ΔT_i for different grating periods $\lambda_i = 2\pi/\xi_{x,i}$ between 500 nm to 20 microns. The decay curves are obtained by calculating the apparent thermal diffusivities versus spatial frequency using Eq. 6 and the phonon dispersion and lifetimes for Si at room temperature as calculated by Jesús Carrete and Natalio Mingo using ShengBTE[22;23] and Phonopy[24] from interatomic force constants obtained with VASP.[25–28] These results are then inserted into Eq. 9, yielding transient decay curves for a particular grating period.

The resulting decay curves, with random noise added of comparable amplitude to that in experiments, are shown in Fig. 1a. We then use the optimization procedure described in
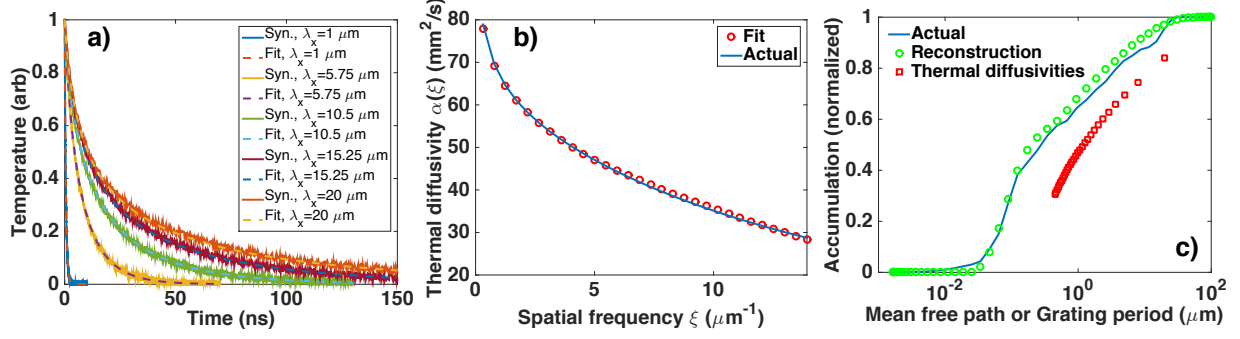
FIG. 1: (a) Synthesized temperature decay curves (solid lines) and decay curves corresponding to the thermal diffusivity function reconstructed by nonlinear optimization (dashed lines). The reconstructed thermal decays are in good agreement with the original synthesized curves. (b) Reconstructed thermal diffusivity $\alpha(\xi)$ (symbols) compared to the actual function (solid line). The reconstructed function is in good agreement with the actual function. (c) Reconstructed MFP spectrum (green circles) using the thermal diffusivity result from (b) (red squares). The x-axis corresponds to MFP for the MFP spectrum or the grating period for thermal diffusivity data. The reconstructed MFP spectrum and the actual distribution (solid line) agree well with each other.

the previous section to reconstruct the apparent thermal diffusivities. For this problem, we discretized the spatial frequencies ξ_i into $M = 30$ equally spaced points, and attempted to fit $N = 25$ temperature decay curves. The extinction coefficients in the cross-plane direction are taken to be $\beta_1 = \beta_2 = 1/500$ nm^{-1}.

In the first set of results, we take the minimum grating period to be 500 nm, a smaller value than is typically achieved experimentally but still possible with commercially available optics. The availability of data at a grating period that is comparable to the optical decay length is very helpful because the thermal decay corresponds predominantly to the single spatial frequency defined by the imposed grating rather than a spectrum of spatial frequencies as in the general case. As shown in Fig. 1b, the reconstructed thermal diffusivity is in excellent agreement with the actual thermal diffusivity despite the presence of noise in the original temperature decay curves in Fig. 1a.

Using this reconstructed thermal diffusivity function, we then close the problem by performing the convex optimization procedure described in Ref.[7] to recover the desired MFP spectrum. This result is given in Fig. 1c, and shows that the reconstructed distribution

is in good agreement with the actual MFP spectrum. Our approach of solving two inverse problems, starting from the original transient decay curves, is thus successfully able to reconstruct the desired MFP spectrum without any knowledge of the MFPs or thermal properties of the material.

The reconstruction without data at grating periods comparable to the optical decay length is more challenging compared to the first case because in the present situation every decay curve corresponds to a broad spectrum of spatial frequencies. In contrast, in the first case the decay curves for short grating periods correspond primarily to the in-plane spatial frequency, providing a tighter constraint on the solution at high spatial frequency. Additionally, in the present case the rapidly decreasing weighting factors for cross-plane spatial frequency in Eq. 9 cause the decay curves to be insensitive to the thermal diffusivities at high spatial frequency, resulting in more uncertainty in the final solution.

Despite these challenges, the reconstruction is still feasible. The reconstructed thermal diffusivity versus spatial frequency obtained when only using grating periods from 1-20 microns is shown in Fig. 2a. The reconstruction and correct answer are in generally good agreement, though a discrepancy exists at high spatial frequencies. Performing the second inverse problem with this input results in a poor reconstruction of the MFP spectrum for values of the MFP below 1 micron (not shown). To circumvent this limitation, we recognize that the reconstructed values for spatial frequencies larger than that corresponding to the minimum grating period, $\approx 2\pi/1 \ \mu m^{-1}$, are only minimally constrained by the available data, and may thus be unreliable. Discarding these points, we perform the reconstruction with the subset of data corresponding to spatial frequencies less than $\approx 2\pi \ \mu m^{-1}$. The result is given in Fig. 2b, demonstrating reasonable agreement with the actual MFP spectrum. Thus, the MFP spectrum can be effectively extracted from 2D TG measurements even if multidimensional heat conduction occurs in all of the measured data. The reconstruction can be made more robust if data with grating period smaller than the optical decay length can be obtained so that the heat conduction is primarily 1D for some of the measurements.

IV. ANISOTROPY OF APPARENT THERMAL CONDUCTIVITY

A recent experimental work reported the anisotropic failure of Fourier's law in a time-domain thermoreflectance (TDTR) experiment in which heat conduction occurs both in- and
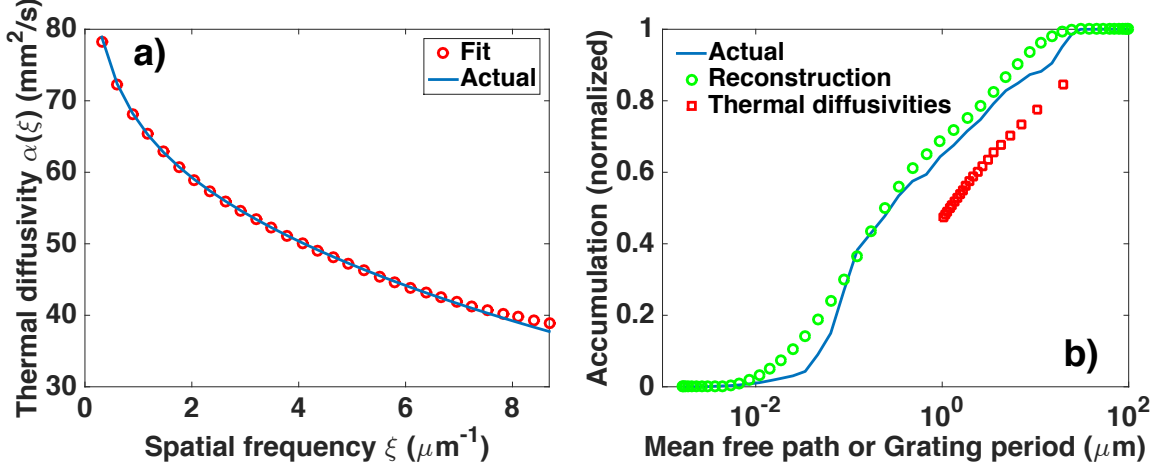
FIG. 2: (a) Reconstructed thermal diffusivity with data from grating periods between 1-20 microns (symbols) compared to the actual function (solid line). The reconstruction is good but a discrepancy exists at higher spatial frequencies. (b) Reconstructed MFP spectrum (green circles) using only the thermal diffusivities in (a) with spatial frequency less than $2\pi \ \mu m^{-1}$ (red squares) compared to the actual spectrum (solid line). The x-axis corresponds to MFP for the MFP spectrum or the grating period for thermal diffusivity data. The reconstructed spectrum agrees well with the actual function provided high spatial frequency data points from (a) are discarded.

cross-plane.[29] The authors observed that the in-plane thermal conductivity of Si appeared to be nearly a factor of two smaller than the cross-plane value when the pump beam diameter was on the order of a few microns, comparable to the phonon MFPs in Si.

Although the samples in the TDTR experiment consist of a film on top of a substrate rather than only a substrate as in TG, we can qualitatively examine this report using our multidimensional solution of the BTE to describe heat conduction in the substrate. First, consider the form of apparent thermal conductivity expressed in Eq. 5. This equation shows that for an isotropic crystal, the apparent thermal conductivity depends only on the magnitude of spatial frequency rather than the components along each direction, implying that the apparent thermal conductivity must be isotropic in real space. Since Si is a cubic crystal that is thermally isotropic, our BTE solution indicates that the apparent thermal conductivity must be isotropic even in the quasiballistic regime regardless of the anisotropy of the thermal gradients.

The obvious question is then why an anisotropic thermal conductivity appears to explain

the data even though the apparent thermal conductivity must be isotropic. A possible answer can be found in the similarity of the Fourier's law solution used to fit the data and the exact solution given by the BTE. Recall from Eq. 9 that the temperature decay of a 2D grating consists of a multiexponential decay with time constants determined by the apparent thermal conductivities that depend only on the magnitude of the spatial frequency. On the other hand, the equation giving the Fourier's law solution for an anisotropic thermal conductivity is given by:

$$\Delta T(t, \xi_x) = A' \int_0^\infty \frac{\exp[-(\alpha_x \xi_x^2 + \alpha_y \xi_y^2)t]}{(\beta_1^2 + \xi_y^2)(\beta_2^2 + \xi_y^2)} d\xi_y \tag{11}$$

where α_x and α_y are the thermal diffusivities along the x and y directions, respectively, and are used as fitting parameters to fit the measured thermal decay. Consider the similarities between Eqs. 9 and 11. In Eq. 9, the integral contains a spectrum of thermal diffusivities that continuously vary with spatial frequency ξ. In Eq. 11, there are only two thermal diffusivities but these separately multiply ξ_x and ξ_y. Due to the averaging caused by the integral over ξ_y, it is possible to reproduce a transient thermal decay by appropriately adjusting α_x and α_y even though this anisotropic solution is inconsistent with the actual BTE solution.

As an example, we calculate the thermal decay derived from the BTE using Eq. 9, then attempt to fit this decay curve using Eq. 11 with α_x and α_y as fitting parameters. For $\lambda = 20$ μm and $\beta = 1/500$ nm^{-1}, we are able to fit the thermal decay nearly exactly using $\alpha_x = 0.85\alpha_{bulk}$ and $\alpha_y/\alpha_x = 0.86$ as shown in Fig. 3. However, this successful fitting does not imply that the apparent thermal conductivity is anisotropic, but rather highlights that multiple solutions can explain the same data for this ill-posed problem. This observation demonstrates the utility of having the exact analytical solution to the multidimensional BTE as presented here.

Our result shows that anisotropic thermal gradients in bulk isotropic crystals are not sufficient to yield apparent thermal conductivities that are anisotropic. It is possible that an anisotropic heating profile, in combination with the metal-semiconductor interface present in TDTR, could lead to anisotropic apparent thermal conductivity; further study with a BTE solution that incorporates the interface is necessary to completely resolve the issue.
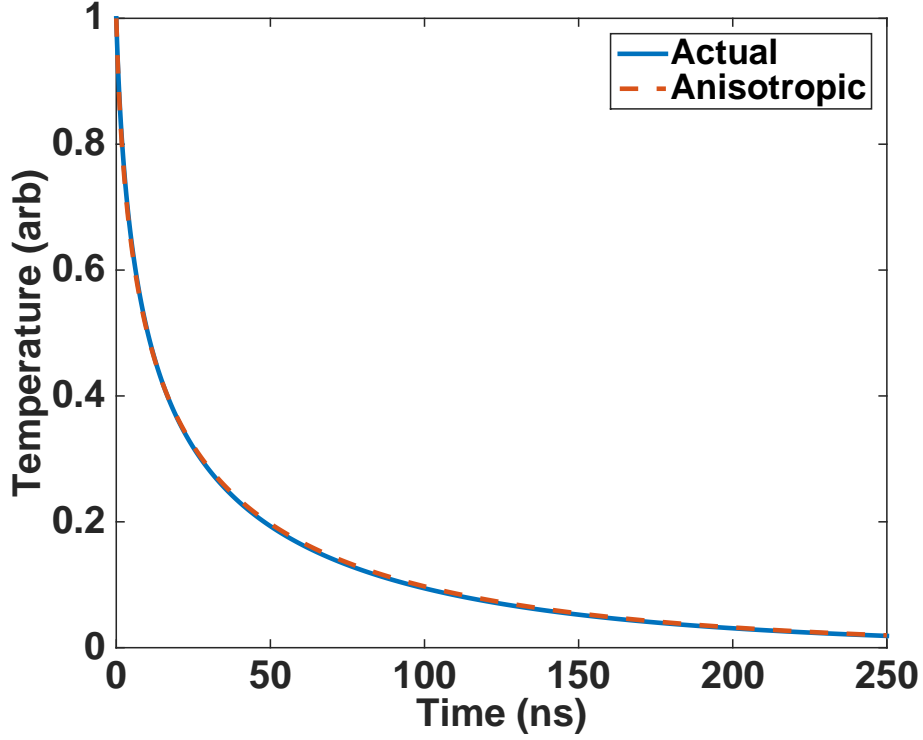
FIG. 3: Calculated temperature versus time from the BTE solution (solid line) and from an anisotropic Fourier model (dashed line). The anisotropic Fourier model is able to explain the observed thermal decay even though the apparent thermal conductivity is isotropic.

V.   SUMMARY

We have analyzed multidimensional quasiballistic thermal transport in TG using an exact analytic solution of the BTE. We find that the thermal decay in multidimensional TG consists of a multiexponential decay with the time constants determined by the apparent thermal conductivities as a function of spatial frequency. By solving a nonlinear inverse problem, we are able to recover these apparent thermal conductivities and thereby obtain the MFP spectrum of the thermal phonons without any fitting parameters or knowledge of the MFPs. This work extends the MFP spectroscopy method with TG to opaque bulk materials.

VI. ACKNOWLEDGEMENTS

---

* Electronic address: `aminnich@caltech.edu`

[1] A. A. Maznev, K. A. Nelson, and J.A. Rogers. Optical heterodyne detection of laser-induced gratings. *Optics Letters*, 23(16):1319–1321, 1998. URL `http://ol.osa.org/abstract.cfm?URI=ol-23-16-1319`.

[2] Jeremy A. Johnson, Alexei A. Maznev, Mayank T. Bulsara, Eugene A. Fitzgerald, T. C. Harman, S. Calawa, C. J. Vineis, G. Turner, and Keith A. Nelson. Phase-controlled, heterodyne laser-induced transient grating measurements of thermal transport properties in opaque material. *Journal of Applied Physics*, 111(2):023503–023503–7, January 2012. ISSN 00218979. URL `http://jap.aip.org/resource/1/japiau/v111/i2/p023503_s1`.

[3] Yanbao Ma. A two-parameter nondiffusive heat conduction model for data analysis in pump-probe experiments. *Journal of Applied Physics*, 116(24):243505, December 2014. ISSN 0021-8979, 1089-7550. URL `http://scitation.aip.org/content/aip/journal/jap/116/24/10.1063/1.4904355`.

[4] Jeremy A. Johnson, A. A. Maznev, John Cuffe, Jeffrey K. Eliason, Austin J. Minnich, Timothy Kehoe, Clivia M. Sotomayor Torres, Gang Chen, and Keith A. Nelson. Direct Measurement of Room-Temperature Nondiffusive Thermal Transport Over Micron Distances in a Silicon Membrane. *Physical Review Letters*, 110(2):025901, January 2013. URL `http://link.aps.org/doi/10.1103/PhysRevLett.110.025901`.

[5] A. A. Maznev, Jeremy A. Johnson, and Keith A. Nelson. Onset of nondiffusive phonon transport in transient thermal grating decay. *Physical Review B*, 84(19):195206, November 2011. URL `http://link.aps.org/doi/10.1103/PhysRevB.84.195206`.

[6] A. J. Minnich. Phonon heat conduction in layered anisotropic crystals. *Physical Review B*, 91 (8):085206, February 2015. URL `http://link.aps.org/doi/10.1103/PhysRevB.91.085206`.

[7] A. J. Minnich. Determining Phonon Mean Free Paths from Observations of Quasiballistic Thermal Transport. *Physical Review Letters*, 109(20):205901, November 2012. URL `http://link.aps.org/doi/10.1103/PhysRevLett.109.205901`.

[8] Chengyun Hua and Austin J. Minnich. Transport regimes in quasiballistic heat conduction. *Physical Review B*, 89(9):094302, March 2014. URL `http://link.aps.org/doi/10.1103/PhysRevB.89.094302`.

[9] Yee Kan Koh, David G. Cahill, and Bo Sun. Nonlocal theory for heat transport at high frequencies. *Physical Review B*, 90(20):205412, November 2014. URL `http://link.aps.org/doi/10.1103/PhysRevB.90.205412`.

[10] R. B. Wilson, Joseph P. Feser, Gregory T. Hohensee, and David G. Cahill. Two-channel model for nonequilibrium thermal transport in pump-probe experiments. *Physical Review B*, 88(14):144305, October 2013. URL `http://link.aps.org/doi/10.1103/PhysRevB.88.144305`.

[11] Bjorn Vermeersch, Jesús Carrete, Natalio Mingo, and Ali Shakouri. Superdiffusive heat conduction in semiconductor alloys. I. Theoretical foundations. *Physical Review B*, 91(8):085202, February 2015. URL `http://link.aps.org/doi/10.1103/PhysRevB.91.085202`.

[12] Jesse Maassen and Mark Lundstrom. Steady-state heat transport: Ballistic-to-diffusive with Fourier's law. *Journal of Applied Physics*, 117(3):035104, January 2015. ISSN 0021-8979, 1089-7550. URL `http://scitation.aip.org.clsproxy.library.caltech.edu/content/aip/journal/jap/117/3/10.1063/1.4905590`.

[13] Maria N. Luckyanova, Jeremy A. Johnson, A. A. Maznev, Jivtesh Garg, Adam Jandl, Mayank T. Bulsara, Eugene A. Fitzgerald, Keith Adam Nelson, and Gang Chen. Anisotropy of the thermal conductivity in GaAs/AlAs superlattices. *Nano Letters*, August 2013. ISSN 1530-6984. URL `http://dx.doi.org/10.1021/nl4001162`.

[14] Jeremy A. Johnson, Alexei A. Maznev, Jeffrey K. Eliason, Austin Minnich, Kimberlee Collins, Gang Chen, John Cuffe, Timothy Kehoe, Clivia M. Sotomayor Torres, and Keith A. Nelson. Experimental Evidence of Non-Diffusive Thermal Transport in Si and GaAs. *MRS Online Proceedings Library*, 1347:null, 2011.

[15] Chengyun Hua and Austin J. Minnich. Analytical Green's function of the multidimensional frequency-dependent phonon Boltzmann equation. *Physical Review B*, 90(21):214306, December 2014. URL `http://link.aps.org/doi/10.1103/PhysRevB.90.214306`.

[16] Jörg Enderlein and Rainer Erdmann. Fast fitting of multi-exponential decay curves. *Optics*

Communications, 134(1–6):371–378, January 1997. URL http://www.sciencedirect.com/science/article/pii/S0030401896003847.

[17] S. Lawrence Marple. Digital spectral analysis with applications. *Englewood Cliffs, NJ, Prentice-Hall, Inc., 1987, 512 p.*, -1, 1987. URL http://adsabs.harvard.edu/abs/1987ph...book.....M.

[18] S W Provencher. A Fourier method for the analysis of exponential decay curves. *Biophysical Journal*, 16(1):27–41, January 1976. ISSN 0006-3495. URL http://www.ncbi.nlm.nih.gov/pmc/articles/PMC1334811/.

[19] Eugene G Novikov, Arie van Hoek, Antonie J. W. G Visser, and Johannes W Hofstraat. Linear algorithms for stretched exponential decay analysis. *Optics Communications*, 166 (1–6):189–198, August 1999. URL http://www.sciencedirect.com/science/article/pii/S003040189900262X.

[20] L. J. Curtis, H. G. Berry, and J. Bromander. Analysis of Multi-exponential Decay Curves. *Physica Scripta*, 2(4-5):216, October 1970. ISSN 1402-4896. URL http://iopscience.iop.org/1402-4896/2/4-5/015.

[21] Jérôme Idier. *Bayesian Approach to Inverse Problems*. John Wiley & Sons, March 2013. ISBN 9781118623695.

[22] Wu Li, Natalio Mingo, Lucas Lindsay, David A. Broido, Derek A. Stewart, and Nebil A. Katcho. Thermal conductivity of diamond nanowires from first principles. *Phys. Rev. B*, 85:195436, 2012.

[23] W. Li, J. Carrete, NA Katcho, and N. Mingo. ShengBTE: a solver of the boltzmann transport equation for phonons. *Computer Physics Communications*, 185:1747–58, 2014.

[24] Atsushi Togo. *Phonony*, v1.8.5. URL http://phonopy.sourceforge.net.

[25] G. Kresse and J. Hafner. Ab initio molecular dynamics for liquid metals. *Phys. Rev. B*, 48: 13115–13118, Nov 1993. URL http://link.aps.org/doi/10.1103/PhysRevB.48.13115.

[26] G. Kresse and J. Hafner. Ab initio molecular-dynamics simulation of the liquidmetalamorphous-semiconductor transition in germanium. *Phys. Rev. B*, 49:14251–14269, May 1994. URL http://link.aps.org/doi/10.1103/PhysRevB.49.14251.

[27] Kresse G. and J Furthmüller. Efficiency of ab-initio total energy calculations for metals and semiconductors using a plane-wave basis set. *Computational Materials Science*, 6:15–50, 1996.

[28] G. Kresse and J. Furthmüller. Efficient iterative schemes for ab initio total-energy calculations using a plane-wave basis set. *Phys. Rev. B*, 54:11169–11186, Oct 1996. URL http://link.

aps.org/doi/10.1103/PhysRevB.54.11169.

[29] R. B. Wilson and David G. Cahill. Anisotropic failure of Fourier theory in time-domain thermoreflectance experiments. *Nature Communications*, 5, October 2014. URL http://www.nature.com.clsproxy.library.caltech.edu/ncomms/2014/141001/ncomms6075/full/ncomms6075.html.